Shipley, T.H., Ogawa, Y., Blum, P., and Bahr, J.M. (Eds.), 1997
Proceedings of the Ocean Drilling Program, Scientific Results, Vol. 156

22. STRUCTURAL GEOLOGY OF THE DÉCOLLEMENT AT THE TOE OF THE BARBADOS ACCRETIONARY PRISM[1]

Alex Maltman,[2] Pierre Labaume,[3] and Bernard Housen[4]

ABSTRACT

The base of the Barbados accretionary prism is defined by a décollement, which separates material accreting to the Caribbean Plate from underthrusting Atlantic Ocean sediment. A three-dimensional seismic survey has shown the structure to contain intervals of negative polarity, interpreted as representing pockets of overpressured fluid. Consequently, Ocean Drilling Program Leg 156 was designed specifically to investigate the hydrogeological and deformational behavior of the décollement.

Analysis of recovered cores shows the structure to comprise a zone of intensified but heterogeneous deformation, 31 m thick, but 39 m thick if suprajacent breccia and various physico-chemical anomalies are included. The top of the décollement shows a pronounced change in the orientation of magnetic anisotropy, indicating efficient decoupling between the prism and the lower material. Core-scale deformation features consist principally of fracture networks, stratal disruption and, most especially, zones of scaly fabric. On the basis of thin-section and scanning electron microscope/transmission electron microscopy observations, the scaly fabric is fractal-like, with zones of sheared clay wrapping around relatively undeformed lenses, at all scales down to that of the individual particles. The scaly zones, consisting of a combination of a pervasive flattening fabric and distributed slip surfaces, are viewed as S-C structures. These develop as shear strains supplant initial flattening microstructures, which is termed spaced foliation. Continuing shear strain progressively dissects the undeformed lenses to produce an overall zone that becomes more intensely sheared, better defined, and narrower—the difference between drilling Site 949 and the more landward Site 948. Fabric-parallel color changes and mineralized veins testify to the structural influence on fluid migration along the décollement. This takes place in periodic pulses, judging by compound nature of the veins and the inferred intermittent collapse of pores during shear-zone formation. That is, the deformation and drainage of the décollement are highly heterogeneous, both spatially and through time.

INTRODUCTION

Off-scraping of sediments from the Atlantic Ocean floor as it converges with and is subducted beneath the Caribbean Plate gives rise to the Barbados accretionary prism (Fig. 1). The ocean floor forms part of the west-moving American plate, also referred to in this region as the North American or the South American Plate. A volcanic arc further west is manifest as the chain of Lesser Antilles islands. The southerly part of the prism is dominated by sands dispersed from the Orinoco and Amazon Delta systems, but to the north, at a greater distance from this source, a series of bathymetric highs have allowed only a relatively thin veneer of sediments to accumulate. As a result, the prism is wider than 300 km in the south, for example east of Tobago, but is less than 50 km wide in the north where the sedimentary supply is restricted. The prism in the north tapers at an angle of only 2.5° and is being underthrust by a sedimentary section about 500 m thick (Shipley et al., 1994). Although the deepest parts of the oceanic trench exceed 5 km, repeated off-scraping of the sediments into the prism has constructed a sedimentary pile great enough to emerge in one place above sea level—the island of Barbados.

Much attention has been paid to the northern part of the Barbados prism, to a large extent because of the clay-rich nature of the accreted sediments. These contrast with the terrigenous clastic sediments that dominate other well-studied accretionary complexes, such as the Nankai prism off Japan, and help complete a spectrum of lithologic variation. The northern area has excellent seismic coverage; moreover drilling on Deep Sea Drilling Project (DSDP) Leg 78A and Ocean Drilling Program (ODP) Leg 110 has already provided a wealth of data (Biju-Duval, Moore, et al., 1984; Mascle, Moore, et al., 1988). The basic structure of the prism is, therefore, well known (Fig. 2): thrusts spaced roughly 1 km apart, with associated hanging wall anticlines, with a transition arcward to back-thrusts and out-of-sequence thrusts (Bangs and Westbrook, 1991; Brown et al., 1990). The various thrusts coalesce into a sole thrust that defines the base of the accretionary prism, and hence acts as the horizon of slippage between the two plates. This zone of detachment is referred to throughout this article simply as the "décollement."

Recently, it is the interplay between the deformation and dewatering of the accreting complex that has been the subject of interest (e.g. Moore, 1989; Brown, 1994). Faults and, especially, the décollement of the Barbados prism have been inferred to be acting as major channels of fluid flow (Mascle and Moore, 1990). The mechanics of how this happens and any quantitative constraints have, however, remained elusive. For example, one enigma has been how to reconcile the décollement being a fluid-escape conduit with considerable evidence of overpressuring within the zone (G.F. Moore et al., 1995), which suggests that it is acting somehow as a fluid trap.

A further intrigue arose from the three-dimensional (3-D) seismic survey that was carried out prior to ODP Leg 156 drilling. Images of the décollement showed areas of positive polarity of seismic amplitude, but also revealed patches of strikingly negative polarity (Shipley et al., 1994). Whereas the positive polarity reflects a normal downward increase in sediment density, the negative polarity indicates a reversal in the density gradient. The negative signals were interpreted as indicating about ten, meter-thick intervals of overpressured fluid. Positive areas would represent pore-fluids at or close to hydrostatic pressure. With this background, Leg 156 was designed to examine the nature of the basal décollement, and in particular, the structural and fluid processes operating there. In addition to obtaining

[1]Shipley, T.H., Ogawa, Y., Blum, P., and Bahr, J.M. (Eds.), 1997. *Proc. ODP, Sci. Results*, 156: College Station, TX (Ocean Drilling Program).
[2]Institute of Earth Studies, University of Wales, Aberystwyth, Wales, SY23 3DB, United Kingdom. ajm@aber.ac.uk
[3]Laboratoire de Géophysique Interne et Tectonophysique, CNRS-Université Joseph Fourier, BP 53X, 38041 Grenoble Cedex 9, France.
[4]Institute for Rock Magnetism, University of Minnesota, Minneapolis, MN 55455, U.S.A.

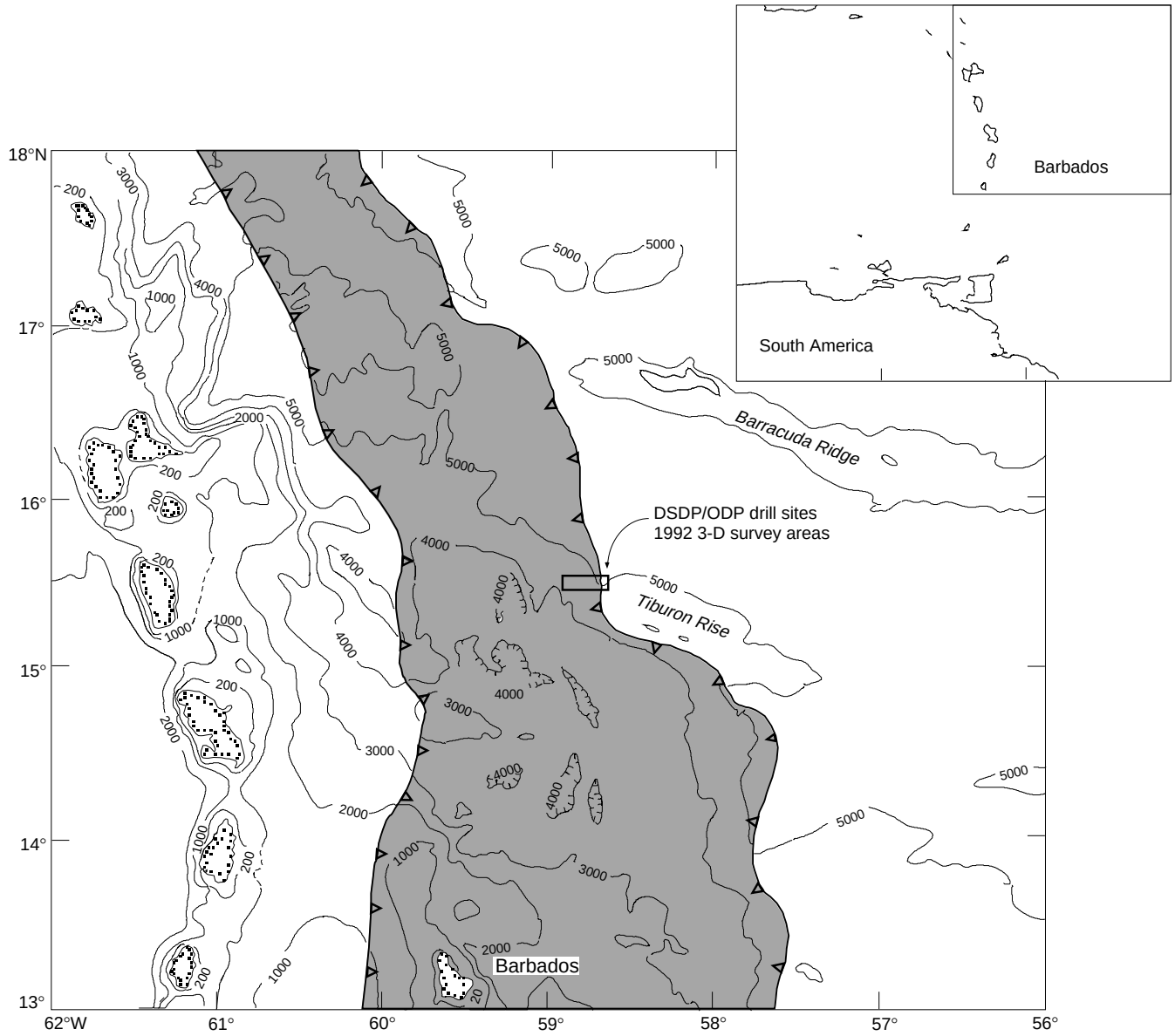

Figure 1. Location map, showing the Lesser Antilles island arc (inset), the island of Barbados, and the extent of the northern Barbados Ridge accretionary prism (shaded). The Tiburon Rise dams along-axis trench transport from the south, causing a narrower prism to the north, dominated by clay-rich sediments. The box shows the location of the DSDP/ODP drilling transects and is approximately the size of the three-dimensional seismic survey carried out prior to the Leg 156 drilling. Bathymetry is in meters (from Shipley, Ogawa, Blum, et al., 1995, fig. 1).

cores for detailed inspection of the décollement, logging while drilling (LWD) was carried out for the first time in an accretionary prism (J.C. Moore et al., 1995), and a series of downhole experiments were performed. Packer tests, for example, succeeded for the first time in this environment in measuring in situ permeabilities (Fisher et al., 1996), and the CORKs were installed to measure possible fluid pressure and geochemical variations through time (Becker et al., Chapter 19, this volume; Foucher et al., Chapter 18, this volume).

Structural geological examination of the recovered cores helped specify the depth of the décollement with greater precision than possible from the seismic sections alone, so that the downhole instruments could be positioned accurately. The observations allowed analysis of the structural nature of the décollement, and provided evidence of the fluid-flow regime in the past. Although the décollement had been penetrated during Leg 110 drilling, which acquired valuable information on the deformation structures (Brown and Behrmann, 1990), much greater time was available during Leg 156 for detailed analysis of the cores, at two separate sites, and this has been complemented by follow-up onshore microstructural analysis. It is now possible to bring together these various strands of investigation into the nature of the décollement, and this article presents that synthesis.

SEISMIC REFLECTION DATA

The results of the 3-D seismic survey have been discussed by Shipley et al. (1994), and a relevant section is illustrated in Figure 3A. The décollement is reasonably clear in the sections, but in the vicinity of Site 949, it loses definition somewhat and takes on the appearance of occupying two horizons. One interpretation is that the lower of the two intervals represents a proto-décollement, which extends eastward beyond the present deformation front (G.F. Moore et al., 1995,

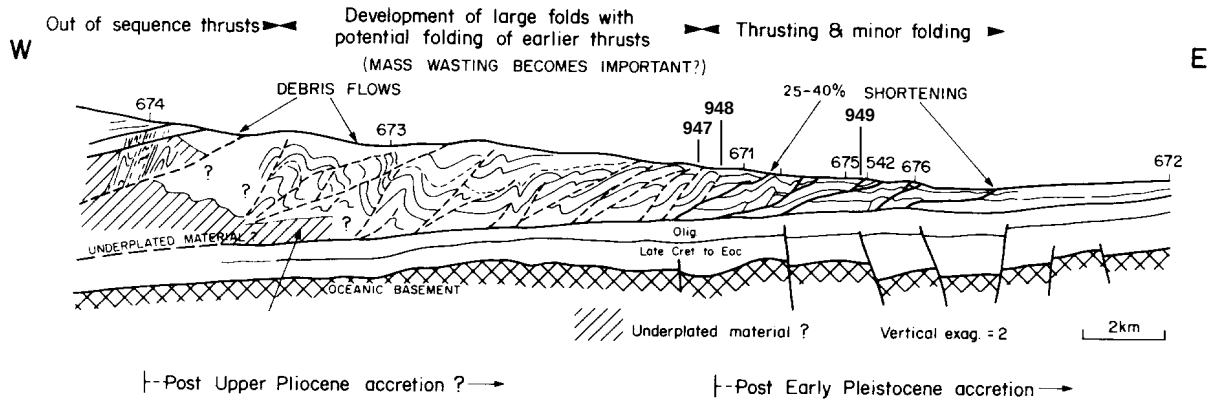

Figure 2. Section interpreted from results of the Leg 110 drilling transect to show the overall structural style of the Barbados prism and the approximate locations (some extrapolated along strike) of DSDP and ODP drilling sites. The décollement separates the accreting Pliocene and younger sediments of the prism from the downgoing Oligocene and older material. See Figures 3A and 10 for a more detailed portrayal of the structure around the décollement. Based on Mascle and Moore (1990), fig. 4.

fig. 12). Thrusts splay upward from the upper horizon, including a diffuse zone which corresponds to the frontal thrust of the prism.

Figure 3B shows a map of seismic amplitude of the décollement reflection. The reverse polarity reflections are scattered over the area, but tend to define a west-south-west alignment. Imaging of the subsediment oceanic crust fails to indicate any basement control on this trend, and its explanation remains elusive. However, results of the Leg 156 drilling substantiated the interpretation of negative polarity areas as pockets of overpressured fluid and led to a better understanding of how this might be taking place (last section).

LITHOLOGIC SITING OF THE DÉCOLLEMENT

The prism toe consists of about 400 m of Quaternary to upper Miocene sediments overlying Miocene claystones (Mascle, Moore, et al., 1988). The Leg 156 coring of the décollement and adjacent sediment led to the recognition of three lithologic units, termed I, II, and III (Fig. 4; Shipley, Ogawa, Blum, et al., 1995). Seismic and core observations show that the décollement zone is centered on and developed along the boundary between Units II and III. Although the lithologies are referred to below as "claystone," all of the sediments in the décollement are poorly lithified to wholly unlithified; all can be cut with a knife. The upper half of the décollement is in the variously colored but dominantly pale, siliceous, pelagic, and hemipelagic claystones of Unit II, whereas the lower half involves the darker, more laminated, turbiditic, and hemipelagic claystones of Unit III. In hand-specimens, the lower unit has a more plastic consistency, and the core-structures suggest the material has deformed in a more ductile manner. It lacks the mineral veins mentioned later and described by Labaume et al. (Chapter 5, this volume). The difference in physical properties may reflect a downward decrease in smectite content, but the visible lithologic contrast between the two units is not great.

It is not obvious why this junction should appear to be localizing the propagation of the décollement. Moreover, in the recovered cores the actual junction is not a site of concentrated strain nor are there visible signs of interleaving of the two lithologic units. The inclination to bedding of some of the recovered shear zones probably means that local, small-scale intercalations occur nearby, but the cored stratigraphic contact itself is undisturbed, and the high-strain zones are developed heterogeneously above and below. Radiolaria reveal, however, that between 510 and 511 m below sea floor (mbsf) and corresponding to deformation zones within the décollement, early early Miocene claystones have been thrust over lithologically similar late early Miocene sediments. Relevant to the fluid-flow behavior of the décollement is the observation that radiolaria in certain intervals within the décollement zone are highly recrystallized, whereas elsewhere they remain intact and well preserved. At one horizon, the radiolaria are cemented and overgrown by quartz, the so-called "fat rad" zone (Shipley, Ogawa, Blum, et al., 1995). The implication of all this seems to be that slip within the décollement zone has remained generally parallel to bedding, without disruption of the stratigraphic sequence. The slip has concentrated fluid flow at certain horizons.

MAGNETIC ANISOTROPY AT THE DÉCOLLEMENT

Results from anisotropy of magnetic susceptibility (AMS) measurements of Leg 156 cores (Shipley, Ogawa, Blum, et al., 1995) demonstrate the ability of the uppermost part of the décollement to decouple the overlying prism sediments from the material below (Fig. 5; Housen et al., 1996). In cores from immediately above the décollement the minimum AMS axes trend nearly east–west and are subhorizontal. Because AMS orientations in deformed sediments usually parallel the principle strains, these axes are indicating horizontal shortening of the prism parallel to the convergence direction of the American plate. The maximum AMS axes are shallowly inclined and nearly north–south trending, parallel to the ocean trench.

At the top of the décollement, however, the orientations of the AMS axes change abruptly. In both the décollement zone and the underthrust sediments the minimum axes are vertical, consistent with the dominant strain being compactional. Although deformation structures are observed in the downgoing sediment, this contrast in AMS orientations suggests that much of the convergence strain is being accommodated by the prism. The abruptness of the change is striking. It indicates that the décollement is capable of efficiently decoupling the converging plates.

MACROSCOPIC STRUCTURES OF THE DÉCOLLEMENT

The cores recovered during the Leg 156 drilling represent the basal décollement of the prism and a few tens of meters above and below the structure (Fig. 4). It is clear that the décollement is a zone of intensification of arrays of deformation features rather than the development of one particular surface or structure. However, one of the most important observations is that the décollement zone is highly heterogeneous. Deformation structures are restricted to certain, spaced intervals, and the remaining parts of the décollement zone are virtually undeformed.

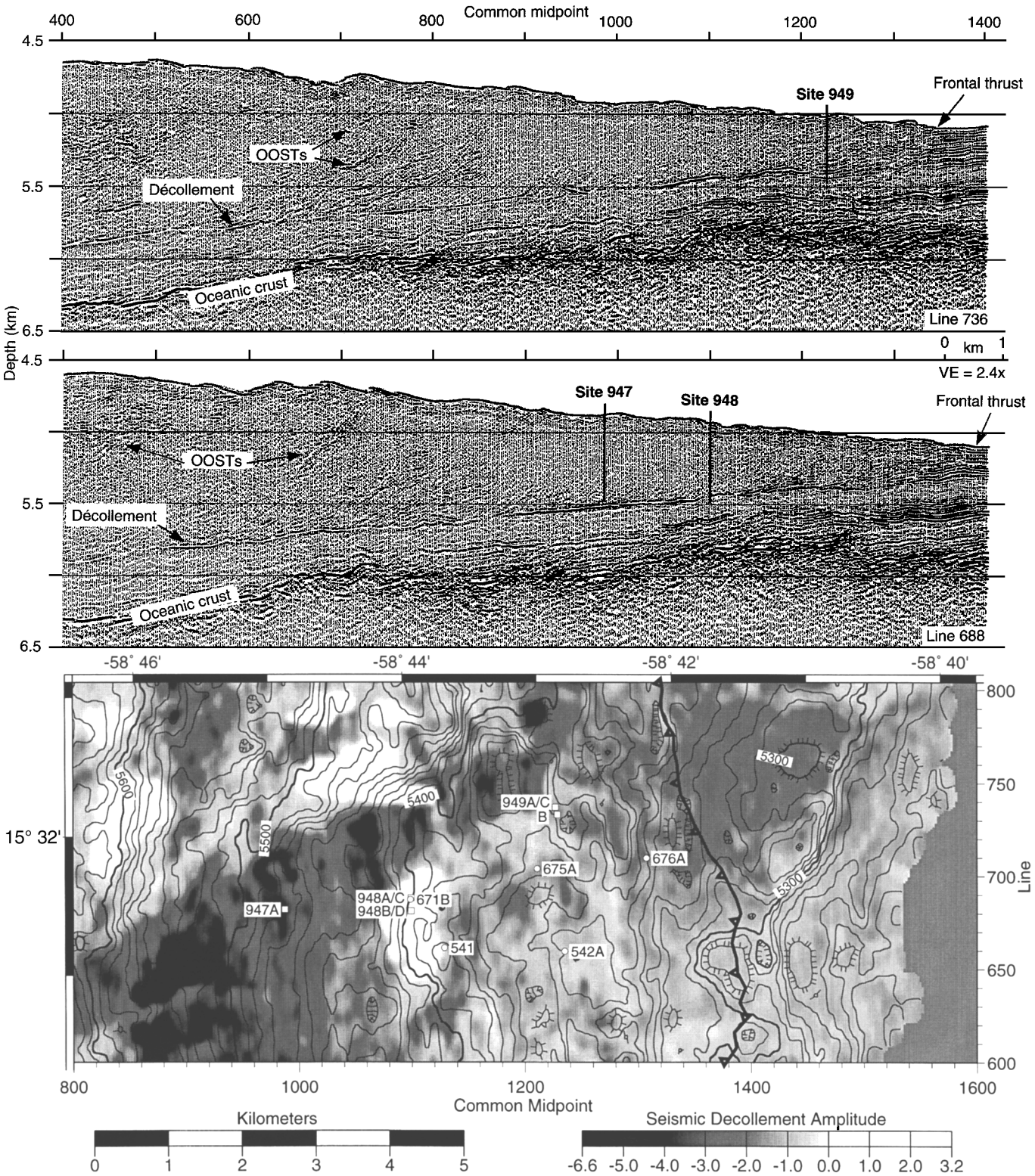

Figure 3. Seismic images of the Barbados décollement. **Top and middle:** depth section taken from three-dimensional seismic survey and corrected using Leg 156 vertical seismic profile velocity data (from G.F. Moore et al. [1995], fig. 6.) **Bottom:** map showing Leg 156 and related drilling site locations and the seismic structure of the décollement. Shading shows the peak seismic amplitude of the décollement reflection; structure contours, at 10-m intervals, show its depth below sea level. Barbed line shows the outcrop on the seafloor of the frontal thrust.

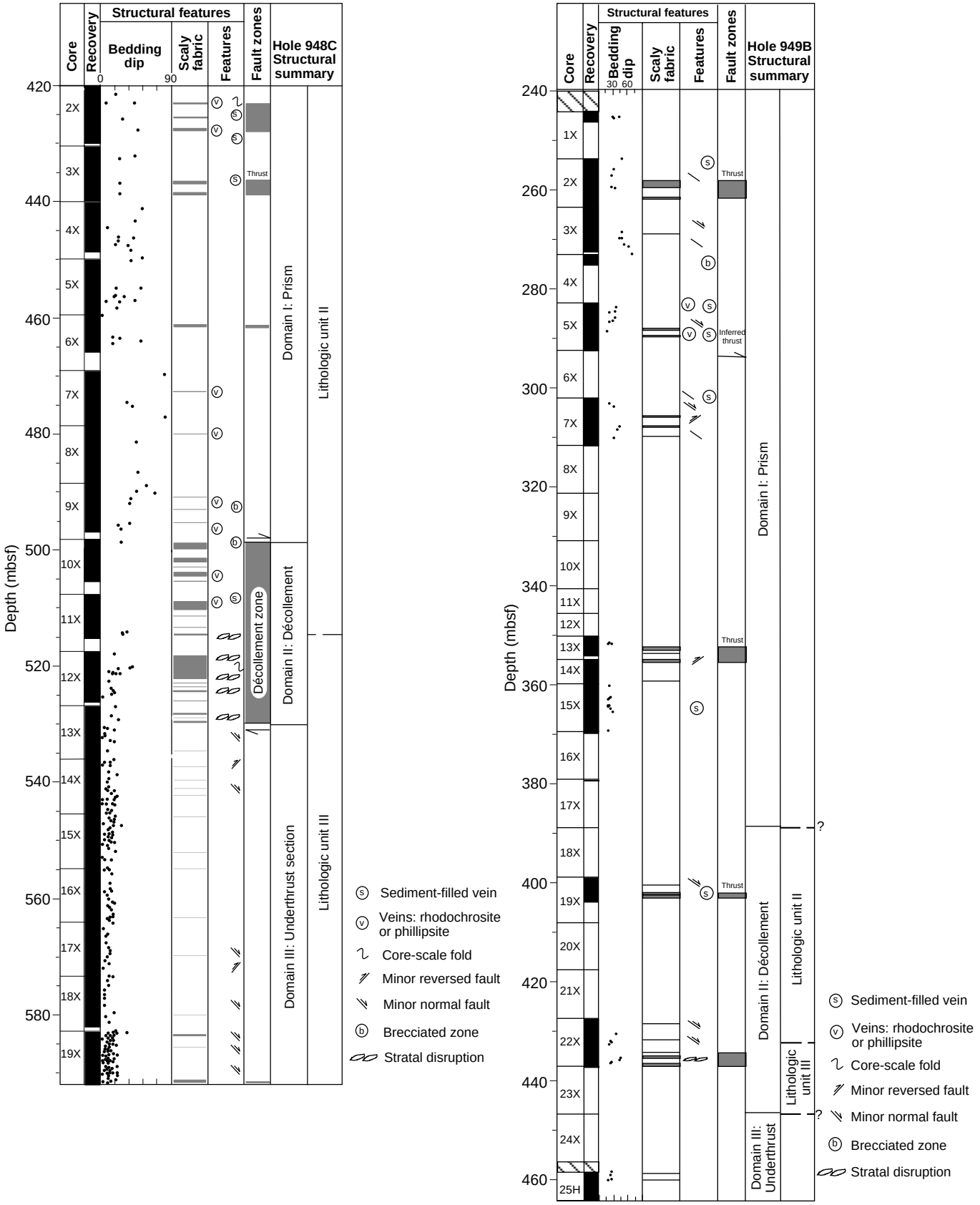

Figure 4. Summary depth log of the main structural features. **Left:** Hole 948C (from Shipboard Scientific Party [1995b], fig. 16). **Right:** Hole 949B (from Shipboard Scientific Party [1995c], fig. 12).

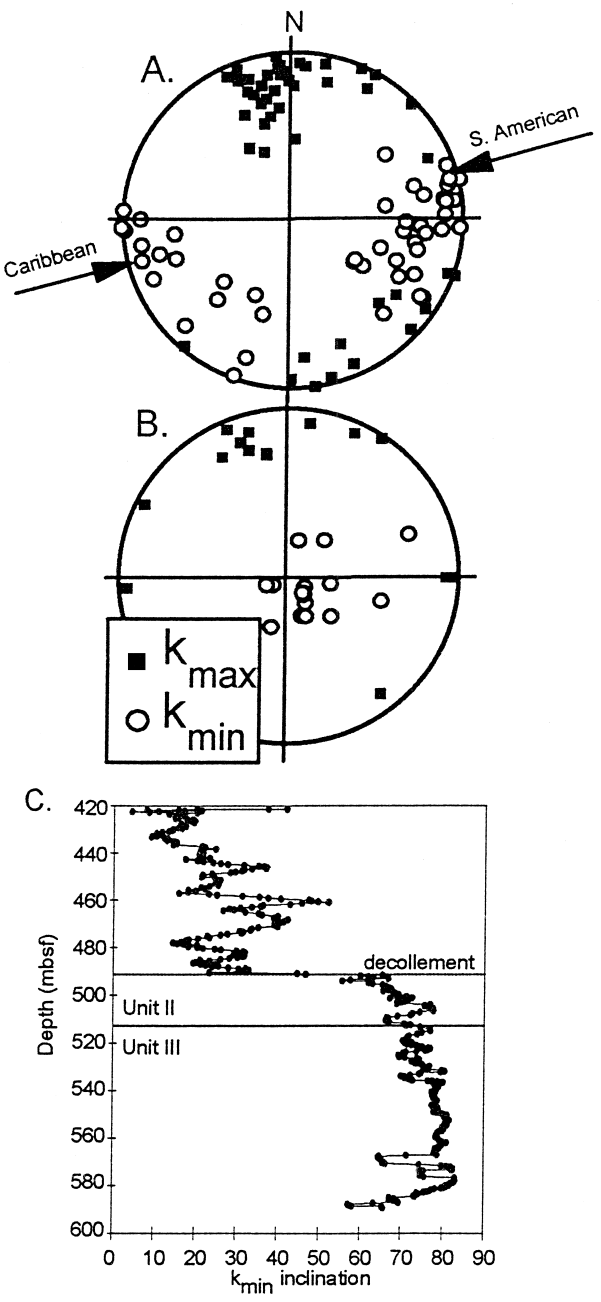

Figure 5. Representative anisotropy of magnetic susceptibility data. **A.** and **B.** Equal area, lower hemisphere projections of reoriented AMS maximum and minimum axes for the lower part of the accretionary prism (**A**) and the décollement zone (**B**). Note the correspondence between the minimum axes, representing the maximum principal strain, and the convergence direction of the Caribbean and South American Plates. **C.** Inclination of the minimum AMS axes, in degrees, vs. depth for sediments cored at Site 948. Note the abrupt change at the upper surface of the décollement zone at 491 mbsf. The boundary between lithologic Units II and III is also shown.

The deformation features in the décollement zone consist chiefly of three types: scaly fabric, fracture networks, and stratal disruption (Fig. 4; Shipley, Ogawa, Blum, et al., 1995). Scaly fabric appears in cores as closely spaced, commonly shiny surfaces that weave around relatively undeformed phacoidal lenses of sediment. Intensely developed scaly fabric is almost planar and typically occurs in zones, referred to in the present work as scaly-fabric zones (Plate 1, Figs. 1, 2). The fabric lies oblique/subparallel to the sharply defined bounding surfaces of the overall zone. The zones themselves are typically a few millimeters to a few centimeters in thickness and are mostly horizontal. Scaly fabric is the most important of the three structures in that it appears to account for the greater part of the shear strain in the décollement zone. It was on the frequency of the scaly-fabric zones that the precise location of the décollement was defined structurally (see next section).

The detail with which we were able to examine the cores made it possible to compute the proportion of the décollement zone occupied by scaly-fabric zones (Fig. 6; Table 1). Taking the interval occupied by the décollement in Hole 948C as 40 m in thickness (see next section), we identified within this 98 zones of scaly fabric. Because each zone occupies a thickness of only a little over 3 cm on average, the total thickness of scaly material is only 3.3 m, or 8.8% of the décollement zone. Most of the scaly zones are horizontal, so any adjustment for apparent thicknesses of inclined zones would have little effect. The other kinds of structures are not included in this calculation, but these are of less importance, and the inference is clear: the deformation in the décollement zone is very heterogeneous.

Adjacent to many of the scaly zones are intervals of criss-crossing surfaces (Plate 1, Fig. 2*)*. During the shipboard observations, we found it increasingly useful to adopt for these a specific name—fracture networks. Each surface appears as a fine, planar crack, although rarely is displacement across them apparent. This is partly because of the sparsity of suitable markers, but also because any shear on one surface is probably minimal. The fractures are typically spaced 5–10 mm apart and occur in interlacing webs without any dominant orientation. The structure is better developed in lithologic Unit II, the upper part of the décollement, and is thought to be the low-strain response of a relatively brittle sediment. It may represent a late stage of deformation (see later).

Stratal disruption may be the analogous response of less brittle sediment to producing fracture networks (Plate 1, Fig. 4). Lithologic Unit III, the lower part of the décollement with its noticeably softer, more plastic feel (see Lithology section), seems to have responded in this way (Fig. 4). Carefully scraping the surface of the split-core faces in places revealed fine sedimentary laminations and bioturbation features that are pulled apart, boudinaged, and offset along narrow, low-angle shear surfaces. Although these last structures are effectively normal faults, the overall deformation appears ductile at this scale of observation. The geometry of these features suggests an extensional response to the overall shear deformation of the décollement. A few folds and reverse faults are seen, but these are rare. Extensional structures predominate, and this helps explain the apparent paucity of repetition and interleaving of horizons mentioned earlier.

These observations represent two important advances on those made during the Leg 110 drilling of the décollement. First, the distribution of the scaly-fabric zones, together with the associated structures now recognized, is not pervasive within the décollement zone but highly heterogeneous. This has important consequences for how continuing strain is accommodated by the zone (see later). Second, sediment-filled veins were previously seen as an important structure of the décollement. Having been observed at Site 672, the reference hole to the east of the deformation front, they were seen as an early manifestation of strain associated with the propagating plate detachment and representative of a proto-décollement. Excellent examples of sediment-filled veins were also recovered from the décollement during the Leg 156 drilling (Fig. 4; Shipboard Scientific Party, 1995c). However, recent work has indicated that this structure is essentially the result, irrespective of the environment, of porous sediment transmitting seismic shear and pressure waves and, in some cases, involving downslope creep (Hanamura and Ogawa, 1993; Brothers et al., 1996). Hence, although sediment-filled veins occur in both the prism and the basal décollement, they are now thought to be unrelated in any direct way to the accretion process.

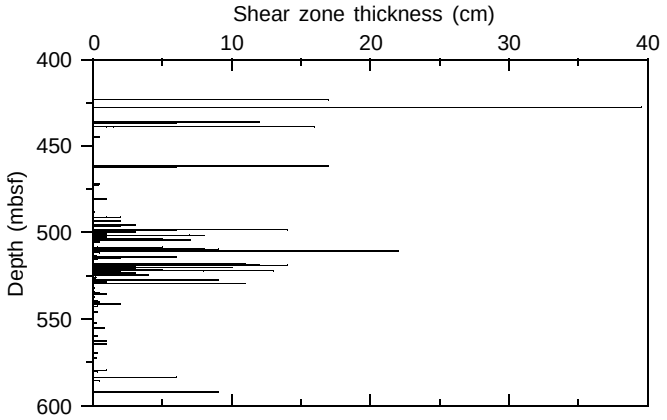

Figure 6. Frequency and thickness of zones of intense scaly fabric (shear zones) in Hole 948C. Note the increased frequency at the décollement zone. The uppermost thick zone (14 cm) of this cluster was taken while shipboard to denote the top of the décollement. Subsequent considerations, see text, suggest that the upper surface of the décollement zone is better defined at the top of the cluster, at 490 mbsf (from Shipboard Scientific Party [1995b], fig. 21).

LOCATION AND ARRANGEMENT OF THE DÉCOLLEMENT

A number of holes were drilled during Leg 156 in association with the various logging procedures and downhole experiments, but the structural geological information about the décollement comes largely from three of them: Holes 948A, 948C, and 949B. The drilling at Site 947 (Shipboard Scientific Party, 1995a) was dedicated to LWD technology, and although this provided invaluable information about the prism it failed to penetrate the décollement (J.C. Moore et al., 1995). Nevertheless, it is highly pertinent that the failure arose because hole conditions about 70 m above the décollement became too unstable to continue drilling, and Site 947 is located at one of the high-amplitude, negative-polarity seismic reflectors thought to represent high fluid pressure. In fact, at the base of the hole, 574 mbsf, the logs indicated a zone with sediment porosities exceeding 70%, about the same as that expected a few meters below the seafloor with normal consolidation. This strong suggestion of high fluid pressure, perhaps approaching the lithostatic value, means that the sediment strength will be reduced almost to zero and explains the drilling difficulties here. The high-porosity zone is interpreted as a thrust plane and, being only some tens of meters above the basal detachment, may represent an upward splay from the décollement. Site 947 therefore indicates, albeit indirectly, that pockets of overpressured fluid exist within and close to the décollement zone.

Site 948 was located as close as possible to Site 671B, which was investigated during Leg 110, where coring had been successful in both the prism and the décollement. Observations from the earlier drilling indicated that the décollement consists of 40 m of intensely sheared scaly clay. Like Site 947, Hole 948A was devoted to LWD, but here, at a site with positive-polarity seismic signature, it successfully penetrated the entire prism, the décollement zone, and over 50 m of underthrust sediment (Shipboard Scientific Party, 1995b). The results disclose important observations for the structural geology of the décollement. Two low-density spikes at 505 and 514 mbsf are thought to indicate porosities of 68% and 61%, respectively, in contrast to material of 53% porosity above the décollement and 47% below (Fig. 7). The lower anomaly spans a 2-m interval and coincides with the Unit II/III lithologic boundary. Inferring such thin (a few meters) intervals of high porosity is very compatible with the distribution of the deformation pattern to be discussed below, although, as remarked above, it is noticeable that the lithologic junction itself shows no deformation in the recovered cores. There is a general downward decrease in density, taken to represent a steady increase in porosity, in the lower part of the prism towards the décollement zone. The lowest value (highest porosity), apart from the two spikes just mentioned, occurs at 494 mbsf, and has a significance that is discussed below.

Table 1. Proportion of scaly fabric zones (SFZ) and undeformed sediment in the décollement zone at Hole 948C, to illustrate the highly heterogeneous nature of the strain.

	Total décollement zone	Lithologic Unit I	Lithologic Unit II
Total thickness (m)	40	24	16
Number of SFZ	98	60	38
Average number of SFZ/m	2.45	2.5	2.4
Cumulative SFZ thickness (m)	3.3	1.8	1.5
Average individual SFZ thickness (m)	0.033	0.03	0.039
% thickness of total	8.8	7.5	9.4

Hole 948C was drilled to 421 mbsf without coring, and then recovery began in order to span the décollement zone (Fig. 4A). The hole was terminated at 592 mbsf, well into the underthrust sediments. Core recovery, at 95%, was excellent and provided a fine opportunity to use the deformation features to define precisely the level of the zone of décollement. The cores showed clearly that the dominant mode of deformation in the sediments is the generation of narrow zones of scaly fabric, with associated fracture networks and stratal disruption as described in the previous section. We carefully recorded the frequency and thickness of these zones (Fig. 6). The marked concentration of scaly-fabric zones coincides approximately with the depth of the décollement seen on the seismic sections at this location and enabled a structural definition of the feature. On this basis, the décollement begins sharply at 498 mbsf and continues heterogeneously for a thickness of about 31 m. The lower margin is gradational at about 529 m. The position of this lower boundary is substantiated by the distribution of the stratal disruption; it is characteristic of the lower half of the zone, below the lithologic junction at 514 mbsf, but is found nowhere below 522 mbsf (Fig. 4A).

Despite the abruptness of the upper boundary as defined by scaly-fabric zones, however, there is some question about exactly how the top of the décollement should be defined. There are a number of observations that suggest the level may be better treated as being a few meters higher. First, the sharp change in anisotropy of magnetic susceptibility at about 490 mbsf has already been noted, suggesting that a horizon exists at this level, where the prism is efficiently decoupled from the lower material. Second, the high-porosity spike at 494 mbsf, noted above, suggests that fluid is concentrated at this horizon. Third, because ideas on fluid flow along the décollement sprang largely from anomalies in chemical concentrations of species such as chloride ion and methane, these were carefully investigated on Leg 156. Such distinct anomalies do occur in Hole 948C, and both occur at 494 mbsf. Fourth, breccia was recorded while shipboard at the top of the structural décollement at 498 mbsf (Fig. 4A; Shipley, Ogawa, Blum, et al., 1995, fig. 20); a further example noted at 492 mbsf together with additional examples seen later above 498 mbsf suggest that this might be an important deformation texture in the uppermost horizons. Parts of these samples are sheared, but some of the clasts show no signs of deformation; the material may be a deformed sedimentary breccia, perhaps later deformed by hydraulic fracturing resulting from overpressure rather than by shearing. Of most significance, the fluid-flow properties of this material are probably different to non-brecciated sediment.

All of this seems to suggest that although the dominant shear strain is being recorded at 498 mbsf and below, important hydrogeological and associated deformation effects are occurring several

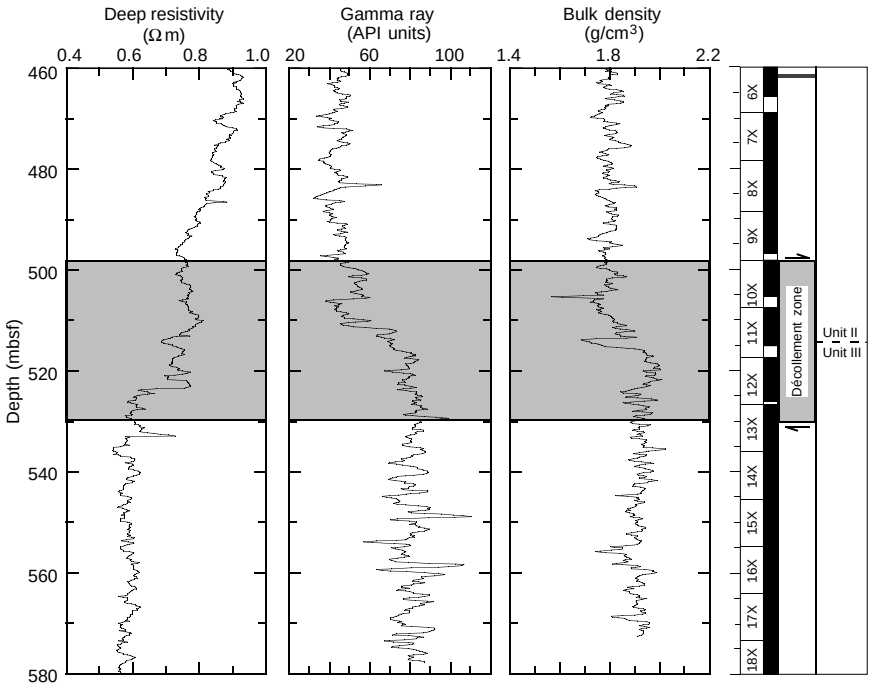

Figure 7. Logging-while-drilling deep resistivity, natural gamma ray, and bulk density logs through the structurally defined décollement at Site 948. Note the low-density spikes, discussed in the text, at 494, 505, and 514 mbsf (from Shipboard Scientific Party [1995b], fig. 66).

meters above this level. Interestingly enough, treating the décollement as a zone between 490 and 529 mbsf gives a thickness of 39 m, virtually identical with the 40 m assigned at nearby Site 671B.

Hole 949B was another attempt to penetrate the décollement at a site of negative-polarity seismic signature (Shipboard Scientific Party, 1995c). The pore-fluid pressures at this site would be expected to be in excess of hydrostatic, but less so than at Site 947, where the seismic wave-form amplitude is greater. In the event, the décollement was successfully drilled, unlike at Site 947, but the core recovery was frustratingly poor, less than 40% (Fig. 4B). Porosities appear to be roughly 5% higher here than in the décollement at Site 948, and presumably even at this site, the fluid overpressuring is sufficient to destabilize the drill hole. Some crucial intervals thought to lie within the décollement zone delivered zero recovery, and only two cores yielded workable data. On the basis of these, the same kinds of deformation features seen at Site 948 are responsible for the décollement, and especially zones of scaly fabric, but the overall intensity of deformation is markedly lower (Fig. 4). The scaly zones are narrower and more widely separated; the décollement zone seems wider and more diffuse. The upper and lower boundaries of the zone are unclear, as is how the core structures relate to the appearance of the two horizons on the seismic records (G.F. Moore et al., 1995, fig. 12). The décollement is at the very least 37 m in thickness at this site, about the same as at Site 948 but could be as much as 90 m. The most likely value is between these two, perhaps encompassing the two décollement-like seismic reflectors.

STRUCTURES OUTSIDE THE DÉCOLLEMENT

The kinds of macroscopic features discussed in the previous sections also occur in sediment outside the décollement zone; it is the frequency of the structures that distinguish the latter (Fig. 4). Plate 1, Figure 3, for example, illustrates the typical appearance of a fracture network in core, but this example comes from 60 m *below* the décollement. Scaly-fabric zones occur throughout the sections away from the décollement, but in restricted intervals, although in a few cases of thicker development they are thought to represent significant faults. A number of the scaly-fabric zones throughout the cored sections have mineralized veins associated with them (Labaume et al., Chapter 4, this volume). These are summarized later, in the context of structural controls on fluid flow.

Perhaps the most striking structural difference away from the décollement zone lies in the orientation of bedding (Fig. 4). There is a little variation within the décollement, as far as bedding can be discerned, and in the underthrust material it is consistently shallow dipping. In contrast, the prism sediments show marked changes in bedding attitude. Shipley, Ogawa, Blum, et al. (1995) report that restoration of bedding orientations in the rotary-drilled cores to their original disposition worked well and allowed various structural subdomains within the prism to be identified.

In summary, the prism sediment is interpreted as the immediate hanging wall and adjacent overlying horizons of the main décollement zone. Several zones of intensified scaly fabric are taken to represent thrusts or oblique ramps splaying from the décollement (Fig. 4). A good example occurs around 437 mbsf at Site 948, where scaly-fabric zones are inclined about 30° and record a reverse sense of displacement. Bedding is steepened and switches to a westward-dip direction, interpreted to reflect thrust-related folding. At other horizons in the prism sediments, bedding dips of 60° and even vertical were noted. At Site 949, a biostratigraphic inversion at around 300 mbsf and a discontinuity in physical properties suggest significant thrusting, but in this case the actual structure must lie in one of the unrecovered intervals. Evidently, and in line with the seismic interpretations (G.F. Moore et al., 1995, figs. 9, 12), décollement-related thrusting has taken place in this hanging wall material, together with folding on the scale of tens of meters.

The underthrust section shows consistently shallow-dipping bedding with a few narrow intervals of scaly fabric (Fig. 4). Some localized faulting probably pre-dates accretion. With the exception of around 590 mbsf at Site 948, where several tens of centimeters of scaly fabric represent a noteworthy low-angle shear zone, though of unknown sense, the indications are that the underthrust material has experienced little deformation related to the plate convergence.

MICROSTRUCTURES OF THE DÉCOLLEMENT

As discussed above, the décollement zone is dominated by and largely defined by zones of scaly fabric. This feature was, therefore,

the chief target of follow-up microstructural investigations, and these are reported in Labaume et al. (Chapter 4, this volume). The chief points are summarized here.

Moving from macroscopic to microscopic observation, using differing degrees of magnification, reveals that the scaly fabric maintains the same appearance at different scales. Core-scale zones of intense scaly fabric are seen in thin section to include smaller phacoids of undeformed sediment. In turn, these scaly zones transpire at the electron microscope scale of observation to contain yet smaller phacoids. Only at the transmission electron microscopy (TEM) scale, where the grains themselves are discernible, is the ultimate texture apparent. In other words, at all scales above that of the individual particles, the scaly fabric of the décollement is highly heterogeneous.

The various microscopic scales of observation show that the macroscopic scaly fabrics correspond to a combination of three types of elemental microstructural features in which strain is localized into micrometer- to millimeter-thick deformation bands. Two of the varieties, spaced foliation and fracture networks, are summarized below. The third type is highly analogous to the S-C bands of ductile shear zones in metamorphic rocks and the like (Berthé et al., 1979; Lister and Snoke, 1984), and can be analyzed in those terms (Plate 2, Figs. 1, 2; Labaume et al., Chapter 4, this volume). An S-C relationship can be surmised in scaly-fabric zones at the core-scale (Plate 1, Fig. 1), but it is at the microscopic scale, both optical and electron microscopic, where it becomes compelling. The S-foliation is a reasonably pervasive alignment of clay particles, somewhat sigmoidal and inclined to the C-surfaces. The latter are extremely narrow foliae of tightly packed, parallel clay particles. The zones are bounded by C-surfaces, although some of the latter also weave through the overall zone.

Microscopic analysis has revealed a significant structure not apparent macroscopically, and for it we use the descriptive term spaced foliation. This is an array of variably spaced, very narrow domains of clay alignment, commonly near to an S-C band, but inclined at a high angle to it (Plate 2, Fig. 3). The domains can be fairly straight and parallel, but appear to become more curvi-planar and anastomosing in more intensely deformed sediment. The extreme preferred alignment within these very narrow domains, even at the margins, suggests that these are primarily flattening rather than shear features. It appears that continuing shear strain prompts the domains to be utilized as shear surfaces, as more intensely deformed examples can show an adjacent sigmoidal fabric, and the whole seems to grade into S-C microstructure. Thus, it appears that the spaced foliation is a precursor of the S-foliation (Fig. 8), although the latter may conceivably evolve in other ways also.

Fracture networks also appear at the microscopic scale and are analogous to those seen in the cores (Plate 2, Fig. 4). Although in places the networks occur alone, most commonly they appear at the periphery of well-developed S-C bands. The network aspect is produced by intensified shear along the spaced foliation, which prompts a second family of surfaces to appear, with opposite dip. Their relation to the S-C bands is one of C′ surfaces or Riedel shears. Thus there is a suspicion that fracture networks may be able to act as precursors to the S-C arrangement, but nowhere did we see good evidence of this. Rather, the C′ surfaces are best developed close to and within the S-C bands, where they offset the S-C features. It may be that S-C bands propagate outward by developing fracture networks, components of which can displace the pre-existing nucleus.

The microstructural analysis, therefore, helps elucidate the nature of the deformation within and around the décollement. The centimeter-scale scaly-fabric zones noted in the cores as dominating the deformation can be considered as large-scale S-C bands, a combination of a pervasive flattening fabric and distributed slip surfaces, and these are evolving from and developing a range of related features. Although it was useful for the purposes of core description to identify and tabulate separately the different types of structures, the microscopic analysis emphasizes that they are more realistically viewed as inter-connected features. We see the structures as parts of associations (Labaume et al., Chapter 4, this volume), interacting as the strain progresses (Fig. 8).

Studies of the décollement following the Leg 110 drilling led to the proposal that scaly fabric has no corresponding clay alignment, but is caused by fracturing during unloading of the cores (Agar et al., 1989; Prior and Behrmann, 1990a, 1990b). Clearly, the present observations refute this. The discrepancy is thought to arise through two factors: sampling and electron microscope technique. The new work emphasizes the heterogeneity of the strain in the décollement zone, at all scales. Consequently, it is easy to sample inadvertently a phacoid of undeformed material—especially as these are relatively strong—rather than the adjacent scaly fabric. The earlier work employed backscattered scanning electron microscope (SEM) analysis alone. We found it difficult to polish a specimen sufficiently to resolve the clay alignments well with this technique, although it was possible (Labaume et al., Chapter 4, this volume, figs. 3C, D, and 4B). But coupling these observations with the greater resolution and the zoom facility of secondary mode SEM and the grain-scale information from TEM, demonstrates clearly that scaly fabric is fundamentally caused by clay reorientation within micrometer- to millimeter-thick deformation bands.

EVOLUTION OF THE DÉCOLLEMENT

The front of deformation at the prism toe is defined by the first thrust, which produces a scarp rising about 100 m from the seafloor and deepening westward to coalesce with the décollement horizon (Mascle et al., 1990). However, judging from the seismic traces and the observations from Hole 672 (the "reference site" drilled eastward of the prism front during Leg 110), there is significant deformation, even discounting the sediment-filled veins (see earlier section) east of this deformation front at around the depth of the base of the prism. AMS data reveal a fabric corresponding to seaward propagating plate–convergence strains in this narrow zone. Unlike the Nankai prism, for example, there is no sign of a "proto-thrust" developing; deformation seems to be focused along a proto-décollement. Our macro- and micro-scale observations have illustrated that in the scaly clay that dominates the deformation zones, the heterogeneity between sheared material and unsheared domains has a similar appearance down to the particle scale, irrespective of the scale of observation. This heterogeneity may continue upward to the scale of the décollement zone itself. The *mode* of deformation appears different at different scales—brittle prism faults involve ductile mechanisms when viewed in detail—but suggest that our model for the development of scaly fabric, deduced mainly from SEM-scale observations, may be used to give the following general scenario for the evolution of the décollement.

The initial strain, oceanward of the prism, is taken up by flattening. AMS data indicate that the prism is undergoing a bulk flattening strain (see earlier section), and we hypothesize that at the proto-décollement a spaced foliation will be developing. The depth at which this occurs will be constrained by the geometry of the converging plates and the thickness of the sedimentary pile, but within this window the strain will be focused along the weakest horizons and at any marked mechanical anisotropies. The latter is presented by the junction between lithologic Units II and III with their differing mechanical properties. Any horizons of breccia or more porous sediment may be storing water unable to permeate the adjacent clays and so may be overpressured and weakened. The spaced-foliation arrays in such locations will eventually yield to shear and, being inclined to the layering, will generate a certain amount of intercalation of the sediments. Although the décollement is centered on the lithologic unit, it will not propagate precisely along it. The spaced foliation, now undergoing slip, becomes more closely spaced and the domains begin to coalesce. Some of them progress into S-C bands and develop peripheral fracture networks/stratal disruption. Scaly-fabric zones develop at the

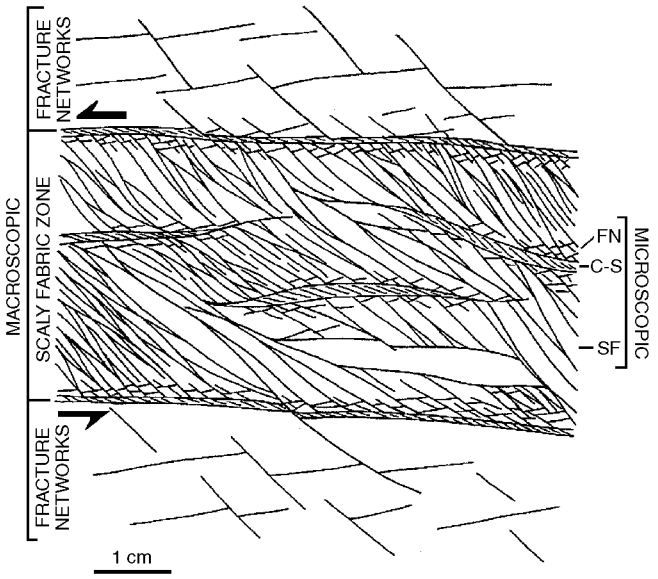

Figure 8. Synoptic sketch to show the associations of microstructures that account for the macroscopic appearance of scaly-fabric zones in cores. FN = fracture network, SF = S-fabric; C-S refers to the S-C deformation bands.

core scale, and, at the next higher scale, the décollement zone intensifies. Densification of scaly-fabric zones in two separate clusters may be responsible for the double décollement inferred at Site 949.

It has been postulated that arrays of shear zones in clays grow by individual surfaces locking up and new zones propagating outward to produce an ever broadening band of sheared clay (e.g. Maltman, 1987; Moore and Byrne, 1987). In the case of the shear-driven detachment at the base of an accretionary prism, the continuing shear strain should, therefore, lead to the décollement thickening landward. Although this may happen after a décollement is pervasively filled by slip surfaces, all the signs are that the décollement at the toe of the Barbados prism is not thickening in this way. Notwithstanding the difficulties of defining the thickness of the décollement at Site 949, the zone becomes narrower and more sharply bounded as it is traced arcward, that is, between Sites 949 and 948. The explanation may lie in the very heterogeneous distribution of the shear. Rather than growing "outward" and thicker, the new shear zones propagate inward into previously undeformed sediment to produce a gradually more intensely and uniformly deformed zone. It may be that once all its internal slip surfaces have been fully utilized the décollement then begins to thicken outward. The fluid-rich zone material around the top of the décollement at Site 948 may become increasingly utilized during subsequent displacement, producing some thickening arcward from the prism toe. These observations emphasize that quantification of the relationship between displacement and thickness of a décollement zone should consider the cumulative thickness of the actual scaly-fabric intervals rather than the bulk thickness of the zone because of the large proportion of unsheared material that it may contain.

There is little doubt that shear zones cannot slip indefinitely (Hicher et al., 1994). Having developed peripheral fracture networks and Riedel shears, perhaps even through-going P-shears, there is increased friction between the now well-aligned particles in a scaly zone, and there are low-tortuosity channels for fluid escape leading to system hardening. The nucleation and propagation of new zones offer an energetically more efficient way of accommodating continuing bulk strain. In addition, any zones experiencing a pulse of elevated pore pressure may propagate through hydrofracture and benefit from reduced frictional strength during the subsequent slip. Thus, the phacoids of undeformed sediment are gradually dissected, shear zone arrays become more closely spaced, and the detachment between prism and underthrust sediment continues, leaving the surrounding material little affected. In this scenario, therefore, the décollement, as seen in Hole 949C, is in its more incipient form, whereas by Hole 948C, it has progressed to a better defined, more mature stage of development (Fig. 9).

The observations summarized in the above sections represent one of only two places in the world where the basal décollement of an active prism has been examined first hand. The other, at Nankai, southwest of Japan, presents some interesting contrasts (see also Karig and Morgan, 1994, p. 203). There, the basal detachment is developed in siltier material and presents a more fragmented appearance, being dominated by breccia and faults. It occupies at the prism toe about half the thickness of the Barbados décollement. Some of the breccia suggests in situ overpressuring, but there are no direct signs of fluid flow. Unlike at Barbados, the Nankai prism may be dewatering diffusely (Maltman et al., 1992). Some further zones of scaly fabric occur in the sediments beneath the décollement of the Barbados prism, but at Nankai the underthrust sediments are almost completely devoid of deformation.

Thus, one of the most striking things in both cases is that the décollement zones are capable of such efficient decoupling between the downgoing material and the overlying prism. Yet these structures, which are acting as major plate boundaries, are only a few tens of meters thick and at Barbados, moreover, the displacement is not distributed throughout the décollement zone, but is focused at specific horizons. Therefore, although most of the deformation structures are recording ductile deformation when viewed at the core and microscopic scales, this restriction of the shear strain to discrete intervals means that any overall view of the décollement gives the appearance of a dominantly brittle mode of deformation. Karig and Morgan (1994) have emphasized the exceptionally brittle style of deformation at Barbados, and regard the basal décollement as a weak, brittle structure that is compatible with implications from the paleomagnetic data (Housen, Chapter 6, this volume) and the low taper angle of the prism (Dahlen, 1990). The décollement, therefore, consists in detail of a narrow zone containing ductile deformation structures, but when viewed at the prism scale is essentially a brittle fault surface.

FLUIDS AND DEFORMATION STRUCTURES

There are several visible signs that fluids have been preferentially concentrated in and around the décollement zone. In general, the zone has a paler coloration than adjacent material, especially in the upper half, where it has a characteristic bright orange look with black blotches of manganese oxide. This coloration effect ignores lithologic banding and appears secondary. Some core-scale scaly-fabric zones show color alteration within them, which in some stops abruptly at the zone boundaries. In the upper part of the décollement, the black manganese oxide patches are in places elongated along the scaly fabric; in one of the most striking specimens recovered from the décollement (Plate 1, Fig. 2), the dark streaks closely follow the aligned clays. In light of the microstructural observations, the appearance shown in Plate 1, Figure 2 would be interpreted as a S-C band, with the manganese oxide preferentially concentrated along both the inclined S-surfaces and some of the bounding C-surfaces. Among the most compelling evidence for fine-scale structural control on the fluid flow within the décollement is the occurrence, within the scaly fabric illustrated in Plate 1, Figure 2, of prismatic crystals of barite, aligned parallel to the S-surfaces and absent from undeformed sediment away from the scaly-fabric zone. As mentioned earlier, a further indication of concentrated fluid flow within parts of the décollement zone is the occurrence of strongly recrystallized radiolaria at certain horizons.

The structural-fluid flow interplay is illustrated strikingly by the occurrence of mineral veins in both the décollement and other fault zones (Fig. 4). They consist mainly of calcium and magnesium car-

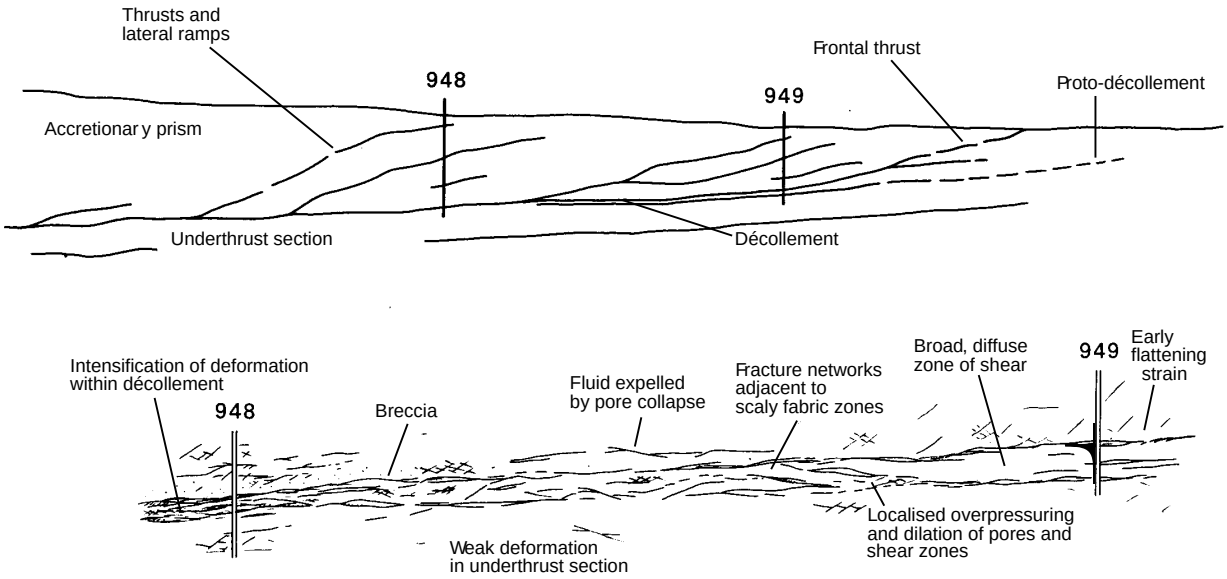

Figure 9. Synoptic sketch to illustrate the structure of the décollement as seen at the two Leg 156 cored sites. Top sketch is based on seismic sections, and the bottom sketch utilizes core-scale and microstructural data.

bonates, but some contain zeolite and phillipsite. Labaume et al. (Chapter 5, this volume) identify four families of veins. One group consists of long, thin, extensional veins that parallel the foliation within scaly-fabric zones. Another family comprises the irregular veins and patches that cross weakly deformed sediment, but are related microscopically to fractures and are always close to scaly-fabric zones. A third type appears unrelated to faulting, but has only been recognized in some loose core-chips, probably originating from the lower part of the prism.

Particularly significant is a fourth group of veins, which show complex, multi-stage microstructures, including evidence of periodic mineral precipitation into open fractures. All the mineral growth shows extensional rather than shear geometry. The manganese content of the fluid appears to have decreased through time, with a corresponding increase in calcium, as the early precipitates are mainly rhodochrosite, whereas the last formed minerals are calcite. The O-, C-, and Sr-isotope contents of the minerals show that the fluids must have originated in the deeper parts of the prism, with decreasing mixing between the exotic and local pre-fluids through time. Such observations, together with the chemical anomalies recorded in the upper part of the décollement, indicate that the décollement zone is capable of transporting fluids over long distances. The compound nature of the veins testifies that the drainage at any place happened intermittently; the texture reflects a history of repeated dilatant "jacking" during progressive deformation and fluid pulsation.

The model presented for the development of scaly fabric (Labaume et al., Chapter 4, this volume) involved porosity collapse following rotation and alignment of clay particles and expulsion of pore fluid. This is one mechanism by which pulses of migrating fluid will be generated. Where the aligned clays do not collapse but are held apart by overpressured pore fluid, the reduction in tortuosity of the flow path will allow the shear zones to act as potential conduits. The same effect will arise where overpressured fluid is injected into a previously formed, but collapsed, scaly-fabric zone. Evidence that this is a significant mechanism comes from the extensional fabric-parallel veins mentioned above. The dilation associated with rotation of the clay particles into their preferred orientation is itself unlikely to have lasted long enough to allow the precipitation of vein minerals. Overpressured pore fluids are, therefore, invoked to prolong the dilation, and the multiple nature of the vein-fill indicates that this happened repeatedly. In addition, there is now laboratory evidence that substantiates and goes some way towards quantifying this "jacking apart" of pre-existing clay alignments (Zwart et al., Chapter 24, this volume).

A general model, therefore, involves the scaly-fabric zones collapsing during their production and generating bodies of expelled fluid. The fluid is overpressured, due largely to tectonic thickening of the prism, and tends to coalesce with other fluid into larger pockets. Bearing in mind the fractal-like aspect of the fabrics, such greater fluid masses may correspond to those detected on the seismic imaging of the décollement. The prism taper gives a hydraulic gradient towards the deformation front, down which the fluid attempts to migrate. The most permeable routes are chosen; these may be embryo scaly zones still in a state of dilation or they may be already formed shear zones of low tortuosity. Such zones will be redilated when the fluid pressure reaches a critical proportion of the confining load (Zwart et al., Chapter 24, this volume), and they will preferentially transmit fluid pulses until the effective pressure rises again. The collapsed scaly zone, perhaps now stained or coated with new mineral, is then available for future re-opening when further pulses of sufficiently overpressured fluid arrive.

The whole scenario is, therefore, one of spatial and temporal discontinuities. At any one time, the deformation will be concentrated at certain intervals and areas of the décollement and, because of its interplay with the fluid escape, the pockets of overpressuring will be highly localized. At a later time, the distribution will have changed. A major result of the Leg 156 drilling and related work is the emphasis that the basal décollement of the Barbados prism is not a zone of uniformly intense and ongoing shear, acting consistently as a channel of steady drainage. Its deformation and hydrogeology are heterogeneous, both spatially and through time.

SUMMARY AND CONCLUSIONS

The structural geology of cores recovered from the décollement at the toe of the Barbados accretionary prism has been analyzed in detail, giving new insight into the nature and evolution of this plate/boundary fault. The structure comprises a zone of intensified but heterogeneous deformation, 31 m thick, but 39 m thick if suprajacent breccia and various physico-chemical anomalies are included. Despite the restricted thickness of such a significant fault, the bulk of the shear strain is concentrated within thin intervals distributed through

the décollement, and these total less than 10% of the overall thickness of the zone. Moreover, the shear fabrics are highly heterogeneous, with zones of sheared clay wrapping around relatively undeformed lenses, at all scales of observation down to that of the individual grains.

Core-scale deformation features consist principally of fracture networks, stratal disruption, and, most especially, zones of scaly fabric. Microscopic examination shows the scaly zones to consist of a combination of a pervasive flattening fabric and distributed slip surfaces, closely resembling S-C structures. These develop as shear strains supplant initial flattening microstructures, termed spaced foliation. Continuing shear strain progressively dissects the undeformed lenses to produce an overall zone that becomes more intensely sheared, better defined, and narrower—the difference between drilling Site 949 and the more landward Site 948.

The top of the décollement shows a pronounced change in the orientation of magnetic anisotropy, indicating efficient decoupling between the prism and the lower material. This is probably facilitated by overpressuring, even though fabric-parallel color changes and mineralized veins testify to fluids migrating preferentially along the décollement. Overpressuring at the décollement implies trapping of fluids there, but this is compatible with facilitated drainage if the processes take place in alternating, periodic pulses. Analyses of the microfabrics of the mineralized veins support this inference and help explain the mechanisms. This, the most detailed examination to date of a décollement zone at an active convergent plate margin, highlights that the deformation and drainage of the structure are strikingly heterogeneous, both spatially and through time.

ACKNOWLEDGEMENTS

Don Fisher and Yujiro Ogawa are thanked for helpful comments on the manuscript.

REFERENCES

Agar, S.M., Prior, D.J., and Behrmann, J.H., 1989. Back-scattered electron imagery of the tectonic fabrics of some fine-grained sediments: implications for fabric nomenclature and deformation processes. *Geology,* 17:901–904.

Bangs, N.L., and Westbrook, G.K., 1991. Seismic modelling of the décollement zone at the base of the Barbados Ridge accretionary complex. *J. Geophys. Res.*, 96:3853–3866.

Berthé, D., Choukroune, P., and Jegouzo, P., 1979. Orthogneiss, mylonite and non-coaxial deformation of granites: the example of the South Armorican shear zone. *J. Struct. Geol.*, 1:31–42.

Biju-Duval, B., Moore, J.C. et al., 1984. *Init. Repts. DSDP,* 78A: Washington (U.S. Govt. Printing Office).

Brothers, R.J., Kemp, A.E.S., and Maltman, A.J., 1996. Mechanical development of vein structures due to the passage of earthquake waves through poorly-consolidated sediments. *Tectonophysics,* 260:227–244.

Brown, K.M., 1994. Fluids in deforming sediments. *In* Maltman, A. (Ed.), *The Geological Deformation of Sediments:* London (Chapman and Hall), 205–237.

Brown, K.M., and Behrmann, J.H., 1990. Genesis and evolution of small scale structures in the toe of the Barbados Ridge accretionary wedge. *In* Moore, J.C., Mascle, A., et al., *Proc. ODP, Sci. Results,* 110: College Station, TX (Ocean Drilling Program)., 229–244.

Brown, K.M., Mascle, A., and Behrmann, J.H., 1990. Mechanisms of accretion and subsequent thickening in the Barbados Ridge accretionary complex: balanced cross-sections across the wedge toe. *In* Moore, J.C., Mascle, A., et al., *Proc. ODP, Sci. Results,* 110: College Station, TX (Ocean Drilling Program), 209–227.

Dahlen, F.A., 1990. Critical taper model of fold-and-thrust belts and accretionary wedges. *Ann. Rev. Earth Planet. Sci.*, 18:55–99.

Fisher, A.T., Zwart, G., Shipley, T., Ogawa, Y., Ashi, J., Blum, P., Brückmann, W., Filice, F., Goldberg, D., Henry, P., Housen, B.A., Jurado, M.-J., Kastner, M., Labaume, P., Laier, T., Leitch, E.C., Maltman, A.J., Meyer, A., Moore, J.C., Peacock, S., Rabaute, A., Steiger, T.H., Tobin, H.J., Underwood, M.B., Xu, Y., Yin, H., and Zheng, Y., 1996. Relation between permeability and effective stress along a plate boundary fault, Barbados accretionary prism. *Geology,* 24:307–310.

Hanamura, Y., and Ogawa, Y., 1993. Layer-parallel faults, duplexes, imbricate thrusts and vein structures of the Miura Group: keys to understanding the Izu forearc sediment accretion to the Honshu forearc. *The Island Arc,* 3:126–141.

Hicher, P.Y., Wahyudi, H., and Tessier, D., 1994. Microstructural analysis of strain localisation in clay. *Computers and Geotechnics,* 16:205–222.

Housen, B.A., Tobin, H.J., Labaume, P., Leitch, E.C., Maltman, A.J., Shipley, T., Ogawa, Y., Ashi, J., Blum, P., Brückmann, W., Filice, F., Fisher, A.T., Goldberg, D., Henry, P., Jurado, M.-J., Kastner, M., Laier, T., Meyer, A., Moore, J.C., Peacock, S., Rabaute, A., Steiger, T.H., Underwood, M.B., Xu, Y., Zheng, Y., and Zwart, G., 1996. Strain decoupling across the décollement of the Barbados accretionary prism. *Geology,* 24:127–130.

Karig, D.E., and Morgan J.K., 1994. Tectonic deformation: stress paths and strain histories. *In* Maltman, A. (Ed.), *The Geological Deformation of Sediments:* London (Chapman and Hall), 167–204.

Lister, G.S., and Snoke, A.W., 1984. S-C mylonites. *J. Struct. Geol.*, 6:617–638.

Maltman, A.J., 1987. Shear zones in argillaceous sediments - an experimental study. *In* Jones, M.E. and Preston, R.M.F. (Eds.) *Deformation of sediments and sedimentary rocks.* Geol. Soc. London Special Publication 29:77–87.

Maltman, A.J., Byrne, T., Karig, D.E., Lallemant, S., and the Shipboard Scientific Party, 1992. Structural geological evidence from ODP Leg 131 regarding fluid flow in the Nankai accretionary prism. *Earth Planet. Sci. Lett.*, 109:463–468.

Mascle, A., Endignoux, L., and Chennouf, T., 1990. Frontal accretion and piggyback basin development at the southern edge of the Barbados Ridge accretionary complex. *In* Moore, J.C., Mascle, A., et al., *Proc. ODP, Sci. Results,* 110: College Station, TX (Ocean Drilling Program), 17–28.

Mascle, A., and Moore, J.C., 1990. ODP Leg 110 tectonic and hydrologic synthesis. *In* Moore, J.C., Mascle, A., et al., *Proc. ODP, Sci. Results,* 110: College Station, TX (Ocean Drilling Program), 409–422.

Mascle, A., Moore, J.C., et al., 1988. *Proc. ODP, Init. Repts.,* 110: College Station, TX (Ocean Drilling Program).

Moore, G.F., Zhao, Z., Shipley, T.H., Bangs, N., and Moore, J.C. 1995. Structural setting of the Leg 156 area, Northern Barbados Ridge accretionary prism. *In* Shipley, T.H., Ogawa, Y., Blum, P., et al., 1995. *Proc. ODP, Init. Repts.*, 156: College Station, TX (Ocean Drilling Program), 13–27.

Moore, J.C., 1989. Tectonics and hydrogeology of accretionary prisms: role of the décollement zone. *J. Struct. Geol.*, 11:95–106.

Moore, J.C., and Byrne, T., 1987. Thickening of fault zones: a mechanism of melange formation in accreting sediments. *Geology,* 15:1040–1043.

Moore, J.C., Shipley, T.H., Goldberg, D., Ogawa, Y., Filice, F., Fisher, A., Jurado, M.J., Moore, G.F., Rabaute, A., Yin, H., Zwart, G., Brückmann, W., Henry, P., Ashi, J., Blum, P., Meyer, A., Housen, B., Kastner, M., Labaume, P., Laier, T., Leitch, E.C., Maltman, A.J., Peacock, S., Steiger, T.H., Tobin, H.J., Underwood, M.B., Xu, Y., and Zheng, Y., 1995. Abnormal fluid pressure and fault-zone dilation in the Barbados accretionary prism: evidence from logging while drilling. *Geology,* 23:605–608.

Prior, D.J. and Behrmann, J.H., 1990a. Backscatter SEM imagery of fine-grained sediments from Site 671, Leg 110 - preliminary results. *In* Moore, J.C., Mascle, A., et al., *Proc. ODP, Sci. Results,* 110: College Station, TX (Ocean Drilling Program), 245–255.

————, 1990b. Thrust-related mudstone fabrics from the Barbados forearc: a backscattered scanning electron microscope study. *J. Geophys. Res.*, 95:9055–9067.

Shipboard Scientific Party, 1995a. Site 947. *In* Shipley, T.H., Ogawa, Y., Blum, P., et al., 1995. *Proc. ODP, Init. Repts.*, 156: College Station, TX (Ocean Drilling Program), 71–86.

————, 1995b. Site 948. *In* Shipley, T.H., Ogawa, Y., Blum, P., et al., 1995. *Proc. ODP, Init. Repts.*, 156: College Station, TX (Ocean Drilling Program), 87–192.

————, 1995c. Site 949. *In* Shipley, T.H., Ogawa, Y., Blum, P., et al., 1995. *Proc. ODP, Init. Repts.*, 156: College Station, TX (Ocean Drilling Program), 193–257.

Shipley, T.H., Moore, G.F., Bangs, N.L., Moore, J.C., and Stoffa, P.L., 1994. Seismically inferred dilatancy distribution, northern Barbados Ridge dé-

collement: implications for fluid migration and fault strength. *Geology,* 22:411–414.
Shipley, T.H., Ogawa, Y., Blum, P., et al., 1995. *Proc. ODP, Init. Repts.*, 156: College Station, TX (Ocean Drilling Program).

Date of initial receipt: 31 July 1996
Date of acceptance: 13 December 1996
Ms 156SR-037

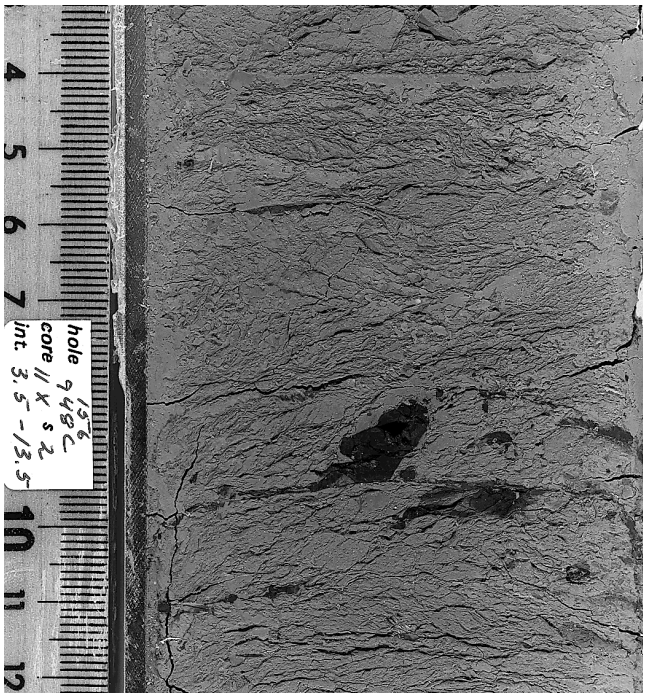

1

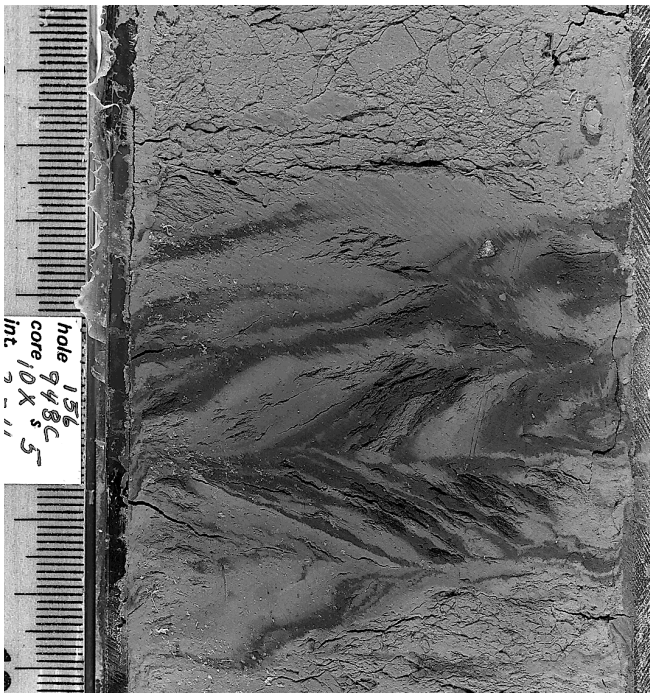

2

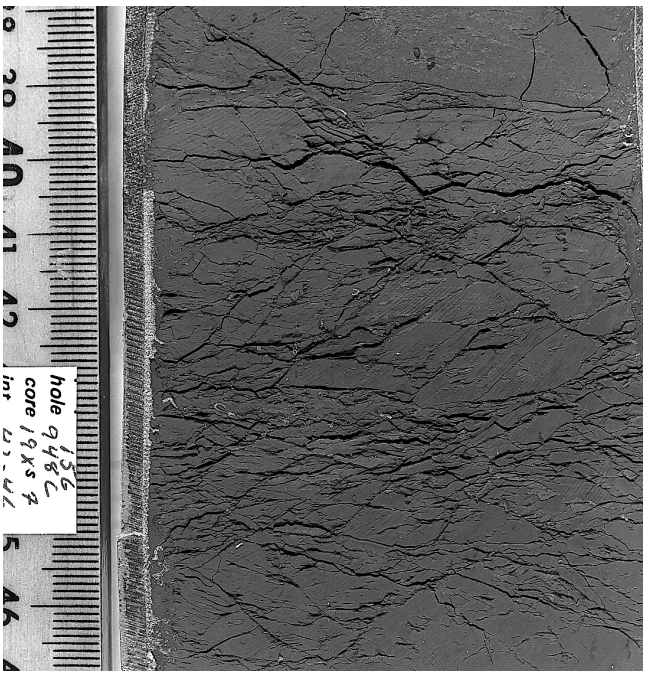

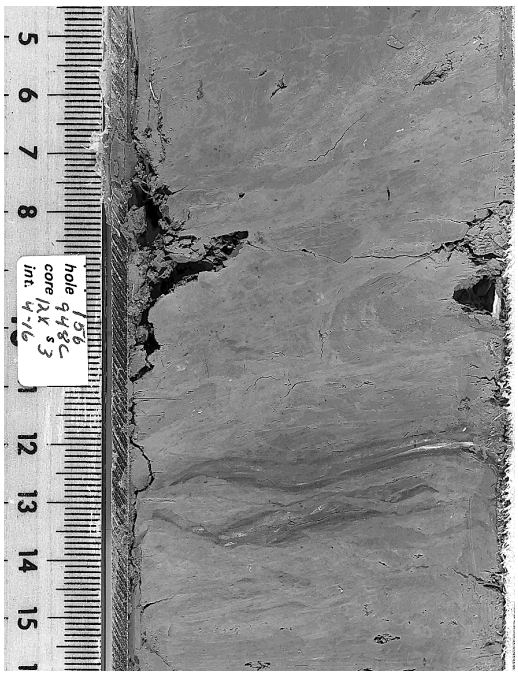

Plate 1. Examples of the main types of structure seen in cores from the décollement. **1.** Scaly fabric, 510 mbsf. Microstructural analysis suggests that the arrangement can be interpreted as an S-C structure, with the inclined, pervasive foliation representing S-surfaces, and the spaced, approximately horizontal domains being the C-surfaces. The dark patches are manganese oxide. **2.** Scaly fabric, from 504 mbsf, showing its close relationship with the distribution of manganese oxide (dark streaks). Structural interpretation as in (**1**). Note that the chevron appearance in this example is illusory: the core has been broken into drilling biscuits that have been differentially rotated by the drilling. **3.** Fracture network, 592 mbsf, in underthrust sediments. **4.** Stratal disruption, 520 mbsf, in Unit III lithology of the lower part of the décollement.

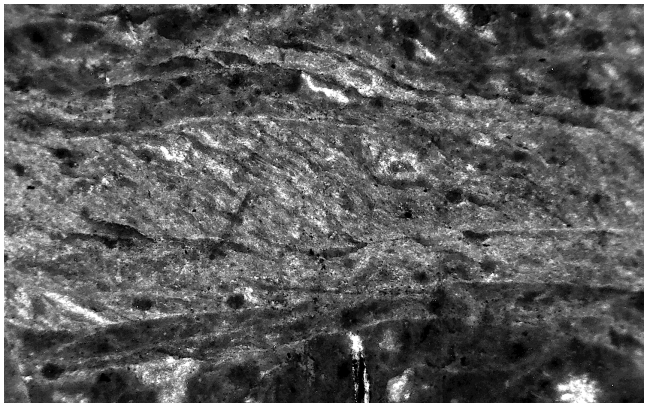

1

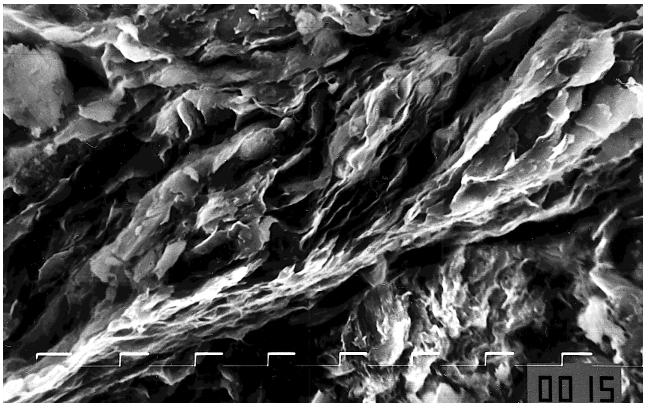

2

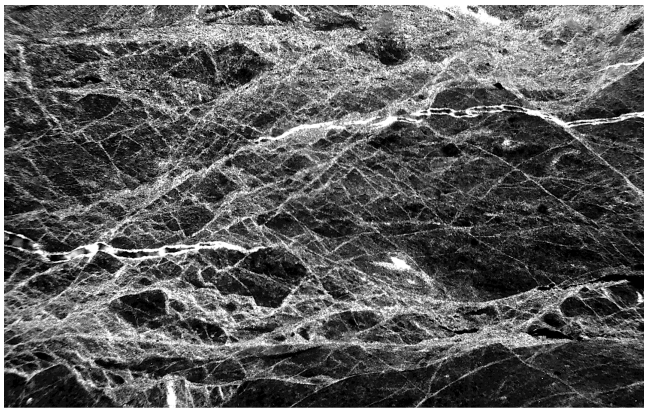

3

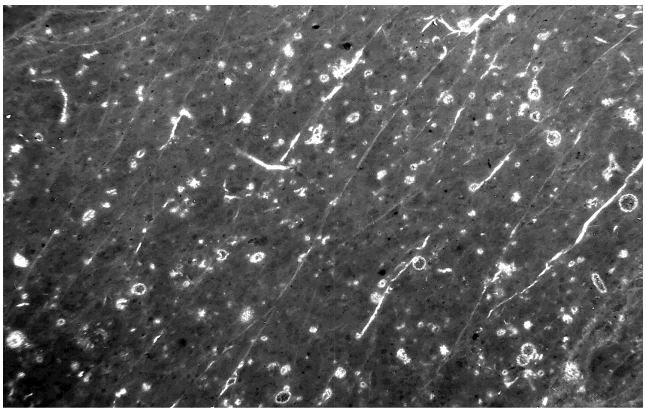

4

Plate 2. Examples of the main types of structure in the décollement at the microscopic scale. **1.** S-C band, in optical photomicrograph. Field of view = 1 mm. Inclined S-surfaces occupy 0.3-mm-thick zone with subhorizontal, very narrow C-surfaces. Geometry implies top-to-the-left sense of movement. Sample 156-948C-11X-2, 68–72 cm; 510 mbsf. **2.** SEM image of S-C band, showing marked preferred orientation of clay particles, pore collapse along C-surface, and varying intensities of preferred orientation and collapse in the S-fabric. Field of view = 200 µm. Sample 156-948C-2X-5, 83–87 cm; 428 mbsf. **3.** Optical photomicrograph of fracture network with cross-cutting deformation bands. Field of view = 4.5 mm. Sample 156-948C-19X-7, 23–27 cm; 592 mbsf. **4.** Optical photomicrograph of spaced foliation. Field of view = 4.5 mm. Structure is at early stage of development, comprising very narrow, relatively planar domains showing no signs of shear. Sample 156-948C-11X-2, 57–61 cm; 510 mbsf.

Previous Chapter Table of Contents Next Chapter